Progress In Electromagnetics Research Letters, Vol. 111, 55–60, 2023

Highly Packaged LTCC Coupler Using Vertically Stacked LC-Elements for 1 and 1.5 Tesla MRI Applications

Linzi Liu, Zheng Pan, Gang Shi, and Bo Zhou*

Abstract—A highly packaged coupler using vertically placed inductors and capacitors (LC)-elements is proposed for 1 and 1.5 Tesla (T) magnetic resonance imaging (MRI) applications. The coupler is made on a 24-layer thickness low temperature co-fired ceramic (LTCC) substrate, and the full integration is reached by heaping up LC-elements in the vertical dimension. The coupler has a smallest reported size of only $0.0035 \times 0.0021 \times 0.001\lambda g$ and a wide fractional bandwidth (FBW) of 44%. The measured in-band phase difference between the coupled and through ports and the amplitude imbalance are less than $91^\circ \pm 0.5^\circ$ and 0.75 dB, respectively. Comparisons and discussions are also implemented.

1. INTRODUCTION

Magnetic resonance imaging (MRI) equipment is an important medical diagnostic device that offers a noninvasive way of imaging with a high sensitivity. 1 Tesla (T) at 42.8 MHz and 1.5 T at 63.9 MHz are the most frequently used working frequencies for scanning [1]. Coupler plays an important role in MRI scanner, which is expected to convert signals between balanced and unbalanced signals with the same magnitude but 90° phase difference. Miniaturization of the coupler is significant as the working frequencies are within the very high frequency (VHF) band.

As the application frequencies are less than 100 MHz, lumped inductor and capacitor (LC)-elements are used for the design for miniaturizations. Recently, many couplers which use lumped elements [2–10] have been reported. Low temperature co-fired ceramic (LTCC) three-dimensional (3D) packaging technique, characterized by having significant advantages in high integration, low cost of mass production, and satisfactory performance, has become the most promising high-density circuit integration technology. Therefore, LTCC fabrication process becomes the first choice in this work. However, couplers in [2, 3] do not fully utilize the LTCC vertical dimensions because of the complicated design process and fabrication cost.

In this paper, a miniaturized and wideband LTCC lumped coupler with satisfied high-packaging characteristics is proposed for 1 and 1.5 T MRI applications at a low center frequency of 54 MHz. Arranging LC-elements vertically superimposed on each other not only meets the need of achieving higher density integration but also shows satisfactory results. By heaping up elements, a further size reduction can be obtained. The final size of the coupler in this work is only $0.0035 \times 0.0021 \times 0.001\lambda g$.

2. DESIGN AND IMPLEMENTATION

2.1. Circuit Topology

The purpose is to make a compact coupler for 1 and 1.5 T MRI applications, which covers the frequencies of 42.8 MHz and 63.9 MHz. Since increasing circuit density and achieving specifications are first

Received 30 April 2023, Accepted 14 June 2023, Scheduled 24 June 2023
* Corresponding author: Bo Zhou (sarahxboy@hotmail.com).
The authors are with the School of Electronic and Optical Engineering, Nanjing University of Posts and Telecommunications, Nanjing 210000, China.

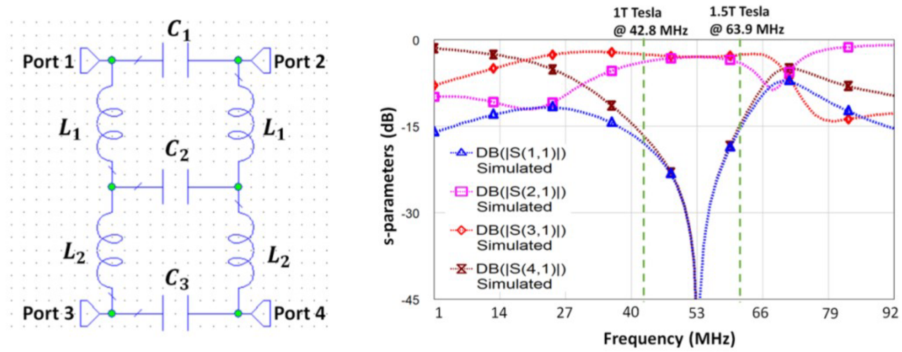

(a) (b)

Figure 1. (a) Circuit topology and (b) its corresponding s-parameters.

priorities, the first step is to select a suitable topology with small quantity of elements. The topology and its corresponding s-parameters are shown in Figures 1(a) and (b), respectively. The proposed topology with 7 elements is composed of 3 center-located capacitors and 4 side-located inductors. Due to symmetry, we can reduce the quantity of optimized parameters, which reduces the burden of simulation. The input, through coupled and isolated port is Ports 1, 2, 3, and 4, respectively. Theoretical values for each element can be obtained by applying Formulas (1)–(2) below:

$$C = \frac{Z_0}{2\pi f} \tag{1}$$

$$L = \frac{1}{2\pi f Z_0} \tag{2}$$

in which f and Z_0 represent the coupler's center operating frequency and the port impedance, respectively. Using Microwave Office Software (MWO) [11], the optimized values are: $C_1 = 50\,\text{pF}$, $C_2 = 48\,\text{pF}$, $C_3 = 49\,\text{pF}$ and $L_1 = 142\,\text{nH}$, $L_2 = 139\,\text{nH}$.

2.2. Vertically Interdigital-Capacitors (VICs) Design

In [2], three capacitors are placed on the same layer, which does no good to integration enhancement and further size minimization. Capacitance can be changed by adjusting VIC's size or tuning the number of VIC's vertical fingers. Therefore, VICs with 8 fingers are selected. In order to make full use of vertical space, three capacitors are stacked up vertically, which greatly increases the density of capacitance. As shown in Figure 2(a), C_1 is on top, C_2 in the middle, and C_3 at the bottom. Also, Figures 2(b), (c), and (d) show planar view with parameter definitions of C_1, C_2, C_3, respectively. Capacitors are interconnected by vias between Layer 8 and Layer 9, Layer 16 and Layer 17. It is worth noticing that, in the actual optimization process, there are slight differences in the size of the three capacitors. The reason for this phenomenon is that each capacitor at different positions has different boundary conditions. Arranging capacitors in the vertical way largely increases vertical integration, thus providing a basis for reducing size. The stimulated capacitances and Q-factors are shown in Figure 2(d). Figure 2(e) shows that the stimulated capacitances of C_1, C_2, and C_3 are 50 pF, 48 pF, and 49 pF, and the stimulated Q-factors of C_1, C_2, and C_3 are 355, 338, and 353, respectively.

2.3. Spiral Inductor Design

Considering that insertion loss is greatly affected by Q-factor, multilayered spiral inductors employ a $W = 0.2\,\text{mm}$ wide line. Square spiral inductors with 11.5 turns are proposed to achieve target inductance. The structure of VICs mentioned above also enhances symmetry and aesthetics. The 3D structure is shown in Figure 3(a). The top view with parameter definitions of $L_1$is shown in Figure 3(b), and the top view with parameter definitions of L_2 is shown in Figure 3(c). L_1 and L_2 are interconnected by via between Layers 12 and 13. Like the phenomenon faced by capacitors, the sizes of L_1 and L_2

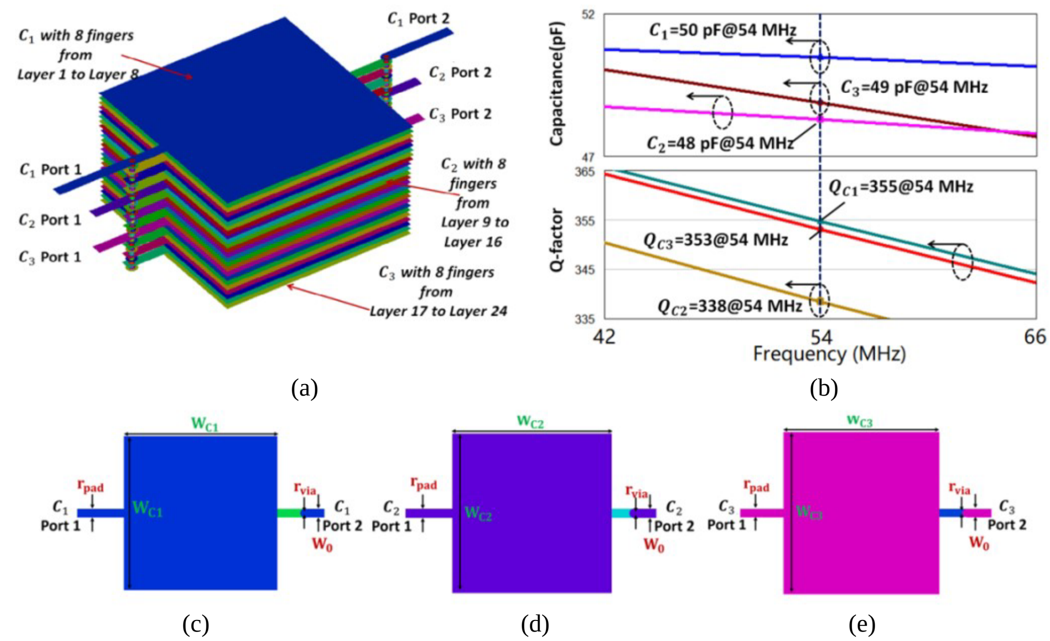

Figure 2. (a) The 3D structure of stacked C1, C2 and C3, (b) Planar view with dimensional parameters of C_1, (c) Planar view with dimensional parameters of C_2, (d) Planar view with dimensional parameters of C_3, (e) EM-stimulated capacitances and Q-factors of C_1, C_2, C_3.

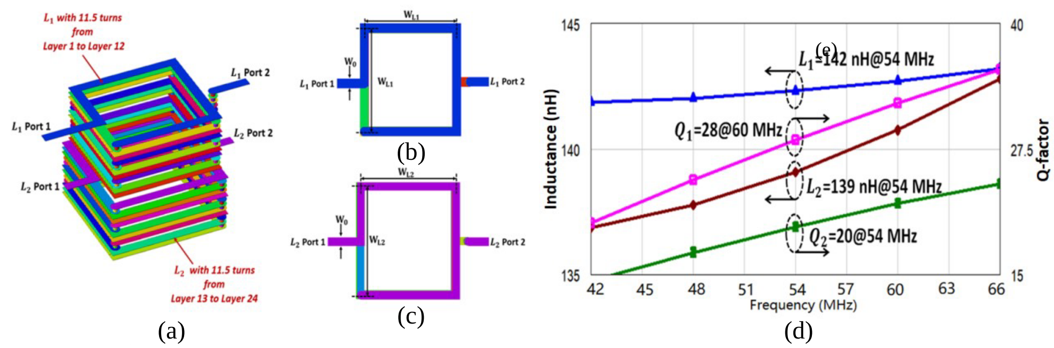

Figure 3. (a) The 3D structure of stacked L1 and L2, (b) Planar view with dimensional parameters of L_1, (c) Planar view with dimensional parameters of L_2, (d) EM-stimulated capacitances and Q-factors of L_1 and L_2.

have fine differences. Like the structure of VICs, multilayered spiral inductors also adopt a stacked-up structure. While taking up smaller areas, larger inductances can be achieved, and more inductors can be built in restricted size. Further integration increment of inductors is achieved, thus promising a further size reduction. At 54 MHz, the stimulated inductances and Q-factors are shown in Figure 3(d). The stimulated inductances L_1 and L_2 are 142 nH and 139 nH, and the stimulated Q-factors of L_1 and L_2 are 28 and 20, respectively.

2.4. Overall Layout Arrangement of the Coupler

With a dielectric constant of 5.9 and a loss tangent of 0.002, the proposed coupler is built within an LTCC substrate with 24 layers, and the 3D structure of the proposed coupler is shown in Figure 4. Each LTCC layer in the Ferro-A6 material has a post-fired thickness of 0.01 mm. The top view and photograph of the proposed coupler are shown in Figures 5(a) and (b), respectively. Three VICs are heaped up in

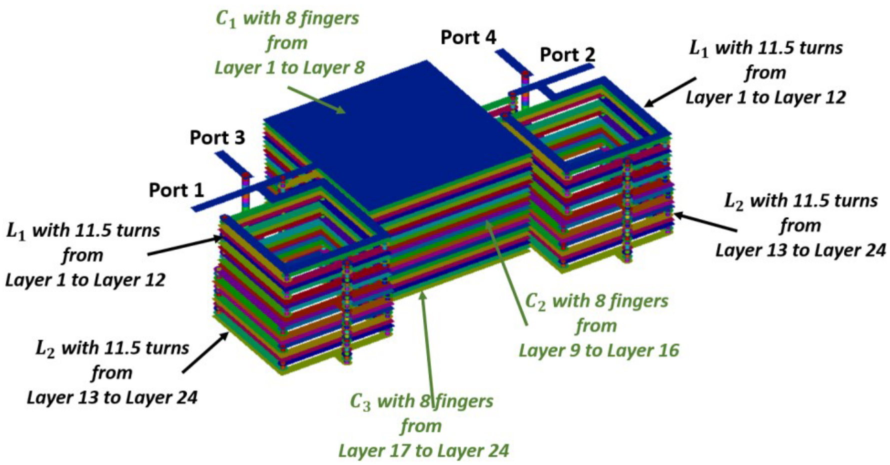

Figure 4. 3D structure of the proposed coupler.

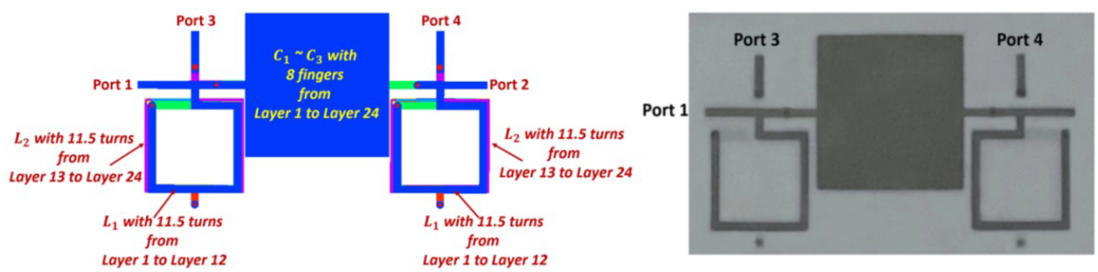

(a) (b)

Figure 5. (a) Top geometry and (b) photograph of the proposed coupler.

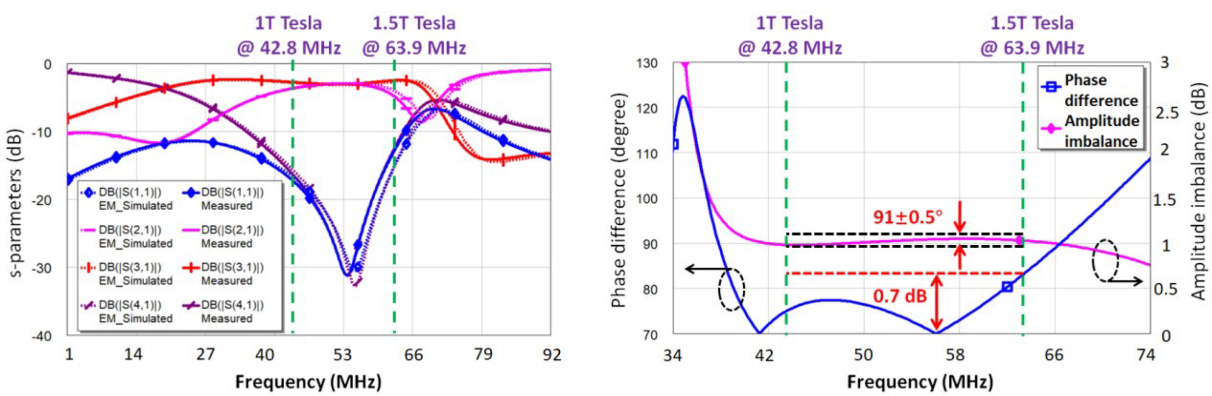

(a) (b)

Figure 6. (a) EM-simulated and measured S-parameters and (b) measured phase difference between the coupled and through ports.

the center. Located at left and right sides of the VICs, the four spiral inductors are in groups of two, and each group consists of two inductors superimposed. By combining all LC-elements, high density packaging is achieved. Final optimal parameters using EM-simulator Analyst [12] are: $W_{C1} = 3.65\,\text{mm}$, $W_{C2} = 3.6\,\text{mm}$, $W_{C3} = 3.8\,\text{mm}$, $r_{pad} = 0.1\,\text{mm}$, $r_{via} = 0.05\,\text{mm}$, $W_{L1} = 2.2\,\text{mm}$, and $W_{L2} = 2.5\,\text{mm}$. The smallest reported size of the introduced coupler in this paper is $0.0035 \times 0.0021 \times 0.001\lambda g$, where λg is the guided wavelength on a Ferro-A6 substrate with a thickness of 2.5 mm at 54 MHz.

3. S-PARAMETERS' SIMULATION AND MEASUREMENT

Figure 6(a) shows simulated and measured s-parameters of the proposed coupler. Measurements are accomplished by Agilent N5230C network analyzer. The measured in band S_{11}, S_{21}, S_{31}, and S_{41} are better than -10 dB, -3.7 dB, -3.4 dB, and -11 dB from 46 to 64 MHz, respectively. Figure 6(b) presents the measured difference between Port 2 and Port 3 which is within $91° \pm 0.5°$, and the amplitude imbalance is below 0.7 dB, showing that it has a fine performance. Using LTCC technology, the circuit in this work achieved a further reduced size compared with other circuits in [2, 4–9], shown in Table 1. Some design issues are worth noticing. First, VICs with the same capacitance have different size because the boundary conditions is different for each VIC. The situation is the same for spiral inductors. Secondly, vias on Layer 8 and Layer 16 should be added between C_1 and C_2, C_2 and C_3 when combining the final LC-elements.

Table 1. Size and performance compararisons.

Refs.	Center frequency (MHz)	Phase Imb (Deg)	Amp Imb (dB)	Overall size (λg)	Process
2	60	91 ± 1	2.8	$0.005 \times 0.004 \times 0.0004$	LTCC
4	1500	90 ± 1	3^a	$0.1385 \times 0.0458 \times 0.0238^a$	SISL
5	4000	180 ± 5	0.7	$0.4 \times 0.28 \times 0.006^a$	LTCC
6	2470	90 ± 0.8	3.39	$0.11 \times 0.006 \times 0.0004^a$	GaAs
7	2050	90 ± 2	4.7	$0.0027 \times 0.0025 \times 1.0714^a$	CMOS
8	10000	90 ± 6	1.5	$0.833 \times 0.037 \times 0.003^a$	MMIC
9	2000	90 ± 5	1.5	$0.39 \times 0.68 \times 0.008^a$	PCB
This work	54	91 ± 0.5	0.75	$0.0035 \times 0.0021 \times 0.001$	LTCC

[a] Data are estimated from the literature.

4. CONCLUSION

Adopting stacked multilayered spiral inductors and VICs, a high density packaged and wideband lumped LTCC coupler is proposed for 1 and 1.5 T MRI applications. Unlike planer structures used in previous works, this work increases freedom of the vertical integration, thus helps obtain further circuit miniaturization. Besides, the structure of the proposed coupler not only meets the higher density integration, but also guarantees satisfactory performances. Working at a center frequency of 54 MHz, the smallest reported size of the introduced coupler is only $0.0035 \times 0.0021 \times 0.001\lambda g$. The coupler also displays a 44% FBW, low in-band phase difference within $91° \pm 0.5°$, and low the amplitude imbalance less than 0.75 dB.

REFERENCES

1. Zhou, Y., P. C. M. van Zijl, X. Xu, et al., "Magnetic resonance imaging of glycogen using its magnetic coupling with water," *Proceedings of the National Academy of Sciences*, Vol. 117, No. 6, 3144–3149, 2020.
2. Zhou, B., W. Sheng, and Y. Zheng, "Miniaturized and wideband lumped LTCC branch-line coupler for dozens of megahertz applications," *Microw. Opt. Technol. Lett.*, Vol. 56, No. 9, 2001–2005, 2014.
3. Zhu, L., "Miniaturized lumped coupler with low frequency signals suppression," *2019 Cross Strait Quad-Regional Radio Science and Wireless Technology Conference (CSQRWC)*, 1–3, Taiyuan, China, 2019.

4. Wang, Y., K. Ma, and S. Mou, "A compact branch-line coupler using substrate integrated suspended line technology," *IEEE Microwave and Wireless Components Letters*, Vol. 26, No. 2, 95–97, 2016.
5. Zhou, B., X. Li, C. Li, L. Qian, and Z. Cai, "Broadband 180° hybrid for 5G applications," *2019 IEEE CPMT Symposium Japan (ICSJ)*, 195–199, Kyoto, Japan, 2019.
6. Ahn, H., I. Nam, and O. Lee, "An integrated lumped-element quadrature coupler with impedance transforming," *IEEE Microwave and Wireless Components Letters*, Vol. 30, No. 2, 152–155, 2020.
7. Frye, R. C., S. Kapur, and R. C. Melville, "A 2-GHz quadrature hybrid implemented in CMOS technology," *IEEE Journal of Solid-State Circuits*, Vol. 38, No. 3, 550–555, 2003.
8. Kazan, O., O. Memioglu, F. Kocer, A. Gundel, and C. Toker, "A lumped-element wideband 3-dB quadrature hybrid," *IEEE Microwave and Wireless Components Letters*, Vol. 29, No. 6, 385–387, 2019.
9. Pan, L., Y. Wu, W. Wang, Y. Zheng, and Y. Liu, "A symmetrical broadband tight-coupled directional coupler with high directivity using three-folded-coupled lines," *IEEE Transactions on Circuits and Systems II: Express Briefs*, Vol. 69, No. 9, 3744–3748, 2022.
10. Hou, J.-A. and Y.-H. Wang, "A compact quadrature hybrid based on high-pass and low-pass lumped elements," *IEEE Microwave and Wireless Components Letters*, Vol. 17, No. 8, 595–597, 2007.
11. Microwave Office, Cadence Corporation, El Segundo, CA.
12. Cadence Analyst, Cadence Corporation, El Segundo, CA.